Spatial-temporal structure of the femtosecond third harmonic generation in photonic-crystal fibers

Vladimir L. Kalashnikov[1]*, Evgeni Sorokin[1], Irina T. Sorokina[2]

[1]*Institut für Photonik, TU Wien, Gusshausstr. 27/387, A-1040 Vienna, Austria*
[2]*Department of Physics, Norwegian University of Science and Technology, N-7491 Trondheim, Norway*

** Corresponding author: kalashnikov@tuwien.ac.at*

Abstract: We analyze the third harmonic generation by the supercontinuum at 1.5 μm in nonlinear-glass microstructured fibers. The numerical model includes the real field dynamics and allows analyzing the spectral as well as the temporal structure of the generated field. The calculated third harmonic and supercontinuum spectra are compared with the experiment in the SF6 glass PCF pumped by a femtosecond Cr^{4+}:YAG oscillator.
The spectral structure of the third harmonic is composed of the 10–20 high-order modes excited at the phase matching points around 500–550 nm. The individual third harmonic modes have spectral widths of 2–4 nm. In the time domain, the third harmonic signal is a ∼10-ps pulse with ps-scale slow modulation, containing subpicosecond ripples at its trailing edge.

OCIS codes: (190.5530) Pulse propagation and solitons; (190.4380) Nonlinear optics, four-wave mixing.

References and links

1. J. M. Dudley, G. Genty, S. Coen, "Supercontinuum generation in photonic crystal fiber," Rev. Mod. Phys. **78,** 1135–1184 (2006).
2. V. L. Kalashnikov, E. Sorokin, I. T. Sorokina, "Raman effects in the infrared supercontinuum generation in soft-glass PCFs," Appl. Phys. B. **87**, 37–44 (2007)
3. R. H. Stolen, "Phase-matched-stimulated four-wave mixing in silica-fiber waveguides," IEEE J. Quantum Electron. **QE-11,** 100–103 (1975).
4. R. H. Stolen and W. H. Leibolt, "Optical fiber modes using stimulated four photon mixing," Appl. Opt. **11,** 239–243 (1976).
5. J. M. Dudley, L. Provino, N. Grossard, H. Mailotte, R. S. Windeler, B. J. Eggleton, S. Coen, "Supercontinuum generation in air-silica microstructured fibers with nanosecond and femtosecond pulse pumping," J. Opt. Soc. Am. B **19,** 765–771 (2002).
6. J. H. V. Price, T. M. Monro, K. Furusawa, W. Belardi, J. C. Baggett, S. Coyle, C. Netti, J. J. Baumberg, R. Paschotta, D. J. Richardson, "UV generation in a pure-silica holey fiber," Appl. Phys. B **77,** 291–298 (2003).
7. C. G. Durfee III, S. Backus, M. M. Murnane, and H. C. Kapteyn, "Ultrabroadband phase-matched optical parametric generation in the ultraviolet by use of guided waves," Opt. Lett. **22,** 1565–1567 (1997).
8. A. M. Zheltikov, N. I. Koroteev, A. N. Naumov, "Self- and cross-phase modulation accompanyning third-harmonic generation in a hollow waveguide," J. Exp. Theor. Phys. **88,** 857–867 (1999).
9. J. K. Ranka, R. S. Windeler, A. J. Stentz, "Optical properties of high-delta air-silica microstructure optical fibers," Opt. Lett. **25,** 796–798 (2000).
10. A. N. Naumov, D. A. Sidorov-Biryukov, F. Giammanco, A. B. Fedotov, P. Marsili, A. Ruffini, O. A. Kolevatova, and A. M. Zheltikov, "Four-wave mixing of picosecond pulses in hollow fibers: phase matching and the influence of high-order waveguide modes," J. Exp. Theor. Phys. **93,** 247–255 (2001).

#83343 - $15.00 USD Received 24 May 2007; revised 19 Jul 2007; accepted 15 Aug 2007; published 22 Aug 2007

11. S. O. Konorov, A. B. Fedotov, and A. M. Zheltikov, "Enhanced four-wave mixing in a hollow-core photonic crystal fiber," Opt. Lett. **28,** 1448–1450 (2003).
12. K. D. Moll, D. Homoelle, and A. L. Gaeta, "Conical harmonic generation in isotropic matherials," Phys. Rev. Lett. **88,** 153901 (2002).
13. T. Schreiber, J. Limpert, H. Zellmer, A. Tünnermann, K. P. Hansen, "High average power supercontinuum generation in photonic crystal fibers," Opt. Commun. **228,** 71–78 (2003).
14. A. N. Naumov, A. B. Fedotov, A. M. Zheltikov, V. V. Yakovlev, L. A. Mel'nikov, V. I. Beloglazov, N. B. Skibina, A. V. Shcherbakov, "Enhanced $\chi^{(3)}$ interactions of unamplified femtosecond Cr:forsterite laser pulses in photonic-crystal fibers," J. Opt. Soc. Am. B **19,** 2183–2190 (2002).
15. F. G. Omenetto, A. J. Taylor, M. D. Moores, J. Arriaga, J. C. Knight, W. J. Wadsworth, P. S. Jt. Russell, "Simultaneous generation of spectrally distinct third harmonics in a photonic crystal fiber," Opt. Lett. **26,** 1158–1160 (2001).
16. N. Y. Joly, T. A. Birks, A. Yulin, J. C. Knight, and P. St. J. Russell, "Linear and nonlinear guidance in an ultralow loss planar glass membrane," Opt. Lett. **30,** 2469–2471 (2005).
17. A. Efimov, A. J. Taylor, F. G. Omenetto, J. C. Knight, W. J. Wadsworth, P. St. J. Russell, "Phase-matched third harmonic generation in microstructured fibers," Opt. Express **11,** 2567–2576 (2003).
18. A. A. Ivanov, D. Lorenc, F. Uherek, E. E. Serebrynnikov, S. O. Konorov, M. V. Alfimov, D. Chorvat, and A. M. Zheltikov, "Multimode anharmonic third-order harmonic generation in a photonic-crystal fiber," Phys. Rev. E **73,** 016610 (2006).
19. A. B. Fedotov, Ping Zhou, Yu. N. Kondrat'ev, S. N. Bagayev, V. S. Shevandin, K. V. Dukel'skiĭ, V. B. Smirnov, A. P. Tarasevitch, D. von der Linde, and A. M. Zheltikov, "The mode structure and spectral properties of supercontinuum emission from microstructured fibers," J. Exp. Theor. Phys. **95,** 851–860 (2002).
20. V. Grubsky, A. Savchenko, "Glass micro-fibers for efficient third harmonic generation," Opt. Express **13**, 6798–6806 (2005).
21. R. A. Sammut, A. V. Buryak, Y. S. Kivshar, "Modification of solitary waves by third-harmonic generation," Opt. Lett. **22**, 1385–1387 (1997).
22. R. A. Sammut, A. V. Buryak, Y. S. Kivshar, "Bright and dark solitary waves in the presence of third-harmonic generation," J. Opt. Soc. Am. B **15**, 1488–1496 (1998).
23. F. G. Omenetto, A. J. Taylor, M. D. Moores, J. Arriaga, J. C. Knight, W. J. Wadsworth, and P. St. J. Russell, "Simulataneous generation of spectrally distinct third harmonics in a photonic fiber," Opt. Lett. **26,** 1158–1160 (2001).
24. F. G. Omenetto, A. Efimov, J. Taylor, J. C. Knight, W. J. Wadsworth, and P. St. J. Russell, "Polarization dependent harmonic generation in microstructured fibers," Opt. Express **11,** 61–67 (2003).
25. A. Efimov, A. J. Taylor, "Spectral-temporal dynamics of ultrashort Raman solitons and their role in third-order harmonic generation in photonic crystal fibers," Appl. Phys. B **80,** 721–725 (2005).
26. E. E. Serebrynnikov, A. B. Fedotov, A. M. Zheltikov, A. A. Ivanov, M. V. Alfimov, V. I. Beloglazov, N. B. Skibina, D. V. Skryabin, A. V. Yulin, J. C. Knight, "Third-harmonic generation by Raman-shifted solitons in a photonic-crystal fiber," J. Opt. Soc. Am. B **23,** 1975–1980 (2006).
27. A. N. Naumov, and A. M. Zheltikov, "Asymmetric spectral broadening and temporal evolution of cross-phase-modulated third-harmonic pulses," Opt. Express **10,** 122–127 (2002).
28. D. A. Akimov, A. A. Ivanov, A. N. Naumov, O. A. Kolevatova, M. V. Alfimov, T. A. Birks, W. J. Wadsworth, P. St. J. Russell, A. A. Podshivalov, A. M. Zheltikov, "Generation of a spectrally asymmetric third harmonic with unamplified 30-fs Cr:forsterite laser pulses in a tapered fiber," Appl. Phys. B **76,** 515–519 (2003).
29. A. Zheltikov, "Multimode guided non-3ω third-harmonic generation by ultrashort laser pulses," J. Opt. Soc. Am. B **22,** 2263–2269 (2005).
30. A. M. Zheltikov, "Third-harmonic generation with no signal at 3ω," Phys. Rev. A **72,** 043812 (2005).
31. G. Genty, P. Kinsler, B. Kibler, J.M. Dudley, "Non linear envelope equation modeling of sub-cycle dynamics and harmonic generation in nonlinear waveguides," Opt. Express **15**, 5382–5387 (2007).
32. A.N. Berkovsky, S.A. Kozlov, Yu.A. Shpolyanskiy, "Self-focusing of few-cycle light pulses in dielectric media," Phys. Rev. A **72**, 043821 (2005).
33. V. L. Kalashnikov, E. Sorokin, S. Naumov, I. T. Sorokina, V. V. Ravi Kanth Kumar, A. K. George, "Low-threshold supercontinuum generation from an extruded SF6 PCF using a compact Cr^{4+}:YAG laser," Appl. Phys. B **79**, 591–596 (2004).
34. E. Sorokin, S. Naumov, I.T. Sorokina, "Ultrabroadband infrared solid-state lasers," IEEE J. Sel. Top. Quantum Electron. **11**, 690–712 (2005).
35. P. Xie, Zh.-Q. Zhang, "Large enhancement of third-harmonic generation induced by coupled gap solitons in $\chi^{(3)}$ nonlinear photonic crystals," Phys. Rev. E **71**, 026610 (2005).
36. G.P. Agrawal: *Nonlinear fiber optics* 3rd ed., (Academic Press, New York, 2001), p 263.

#83343 - $15.00 USD Received 24 May 2007; revised 19 Jul 2007; accepted 15 Aug 2007; published 22 Aug 2007

1. Introduction

Generation of the spectral supercontinuum (SC) in microstructured fibers (photonic crystal fibers, PCFs) has opened new possibilities for the applied nonlinear optics (see [1] and references therein). SC is of interest for a number of applications ranging from spectroscopy and metrology to the medicine. Possibility of the SC generation at unprecedentedly low level of the input pulse energy (sub-nanojoules) in the microstructured fibers results from the enhancement of nonlinearity and long interaction length due to the controllable fiber group-delay dispersion (GDD). The enhancement of the nonlinearity is caused by the strong mode confinement while the GDD control is made possible through the waveguide contribution to the fiber dispersion. As a result of this favorable combination, the spectrum evolution includes, besides the self-phase modulation, also the stimulated Raman scattering (SRS) [2] and generation of new components due to the four-wave mixing (FWM) [3, 4], including the third-harmonic (TH) generation [8, 9].

The waveguide contribution to GDD provides the phase-matched FWM and thereby enhances the efficiency of the frequency conversion [3]. In particular, the required phase matching can result from a stimulated excitation of the high-order waveguide modes in conventional fibers [4] or PCFs [5, 6]. Such a process allows generating the third harmonic in a gas-filled hollow fiber [7, 8] and a PCF [9] by both the direct conversion $3\omega = \omega + \omega + \omega$ and the cascading process $3\omega = 2\omega + 2\omega - \omega$ [10, 11]. It was found that the surface effects, the symmetry breaking and the Cherenkov's type phase-matching (like that in a bulk material [12]) can contribute to the TH generation in a PCF [13, 14]. However, the waveguide contribution to TH in the fibers is a dominant factor in contrast to the bulks. Such a contribution results in a "discreteness" of the TH spectra [15, 16], meaning that the isolated TH spectral lines reproduce the discreteness of the higher-order fiber modes providing a phase-matching with the low-order mode of the pump pulse [17, 18].

The multimode phase-matched FWM was found to be the basic mechanism of TH generation in PCF [17, 18, 19, 20]. Besides the phase- and group-velocity mismatches, the TH spectrum is affected by solitonic effects [21, 22], Raman self-shift [23, 24, 25, 26], polarization of the pump field [24], dispersive-wave generation [26], self- and cross-phase modulation [8, 27, 28]. As a result, the TH spectrum can be broadened, asymmetrical and frequency-shifted from the exact 3ω point [14, 18, 27, 28, 29, 30].

In spite of progress in the investigations of the TH generation in the PCFs, the theoretical analysis concerned mainly the phase-matching effects [17, 14, 18], while the field dynamics remained unstudied. Both analytical [14, 18] and numerical [20] analysis of the TH generation by a non-dispersing pump pulse soliton have been performed. The soliton dynamics (dispersion up to the second order) in the presence of TH generation was described in [21, 22]. Dynamics of the pulse propagation at high peak intensities of $\sim 10^{13}$ W/cm^2 has been investigated numerically [31, 32] beyond the slowly varying amplitude approximation and taking the high-order dispersion into account. For such pulses the nonlinear interaction is very strong and results in efficient TH generation without phase-matching already at distances of 100 μm [31] to 400 μm[32]. In this work we perform the analysis for the real-world conditions of cm-long fibers with high modal and material dispersion and typical low-power oscillator pulse parameters (duration $\sim$10 light cycles and energy $\leq$ 2 nJ, corresponding to peak intensities $\leq 10^{12}$ W/cm^2). Such pulses are conveniently produced by a number of sources and their dynamics substantially differs from high-intensity cases of amplified pulses. We present the results of the numerical analysis of the SC dynamics in the presence of the TH generation provided by the multimode phase-matched FWM. The spatial, spectral and temporal structure of TH is studied theoretically and found to agree with the experimental data for a SF6 glass PCF pumped by a Cr^{4+}:YAG oscillator operating at 60–70 fs pulse duration [33, 34].

#83343 - $15.00 USD Received 24 May 2007; revised 19 Jul 2007; accepted 15 Aug 2007; published 22 Aug 2007

2. Multimode phase matching in a SF6 glass PCF

As demonstrated in Ref. [33], an extruded SF6 PCF with approximately 4.5 μm rectangular core can generate a low-threshold octave-spanning SC when excited by a femtosecond pulse at $\lambda_0 \approx$1.5 μm. This is due to the proximity of the zero-GDD wavelength to 1.5 μm and very high nonlinear refraction in the SF6 material. Large nonlinearity in the combination with the strong mode confinement provides both, efficient FWM and multimode phase matching. As a result, 2ω, 3ω and mixed frequencies can be observed [33]. In this work, we theoretically and numerically analyse the FWM $3\omega = \omega + \omega + \omega$ process in a SF6 PCF and compare it with the experiment.

A typical PCF used for the infrared SC generation is shown in Fig. 1. The mode structure of PCF was analyzed on the basis of the full-vector model using the real core geometry [33]. The fiber is multimode in the infrared, but only the lowest modes M=1–4 (Fig. 1) can contribute to the SC and TH generation because of large shift of the zero-dispersion wavelength for the higher-order modes [33] from λ_0. The rectangular slightly asymmetric PCF core geometry gives rise to slightly different mode parameters depending on polarization [33]. This should result in the polarization effects, but we were unable to observe any noticeable birefringence in the experiment, neither in the SC nor in the TH signal. We suppose that the core inhomogeneity along the fiber (evidenced by the fluctuations of the visible light emission) mixes the polarizations within the first millimeters of propagation.

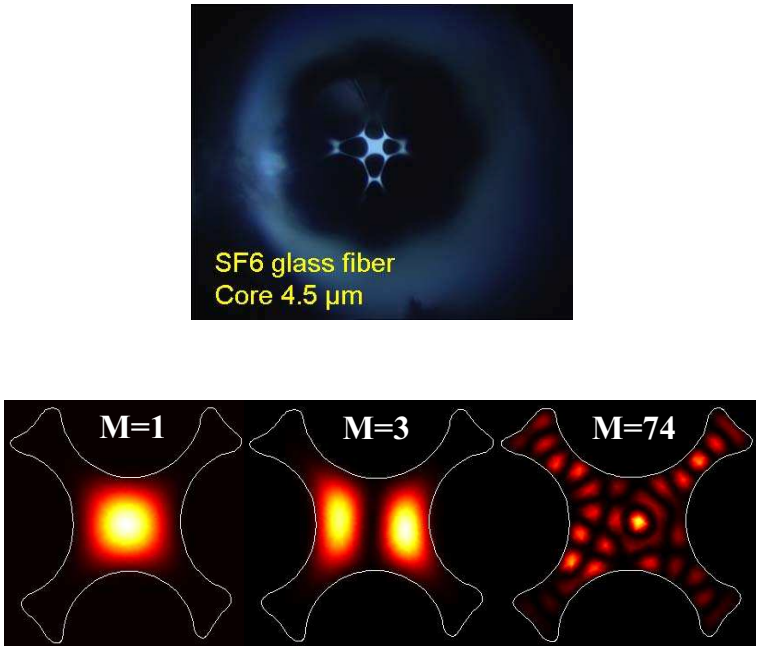

Fig. 1. Cross section of the SF6 PCF (upper graph) and field intensity distributions for the two lowest infrared modes and one visible mode (lower graph, see text for mode designations).

As a result of the waveguiding contribution to the effective refractive index, it is possible to satisfy the phase matching condition: $n_{\mathrm{eff,M}}(\omega) = n_{\mathrm{eff,N}}(3\omega)$, where M and N are the mode indices and $M < N$. Fig. 2 shows the effective refractive indices of the lowest-order modes in the vicinity of λ_0 (M =1, 2) and the high-order modes in the vicinity of $\lambda_0/3$ (N =69–80) as a function of wavelength for the SF6 PCF with a 2.5 μm core. The mode enumeration rule

#83343 - $15.00 USD Received 24 May 2007; revised 19 Jul 2007; accepted 15 Aug 2007; published 22 Aug 2007

corresponds to Ref. [33], so that the two lowest-order modes result from the two orthogonal polarizations of the zero-order PCF mode. The phase matching points are shown by the red circles.

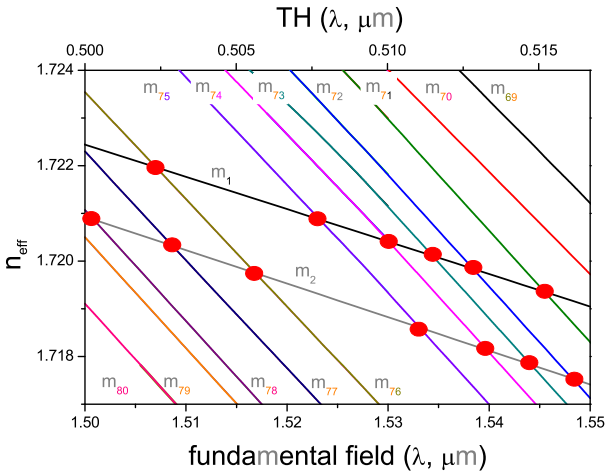

Fig. 2. Effective index of refraction $n_{eff,M}$ at the fundamental wavelength ($\approx \lambda_0$, M =1, 2) and at the third harmonic ($\approx \lambda_0/3$, M = 69–80). Red circles show the phase matching points. SF6 PCF with 2.5 μm core.

The experimental TH spectra were obtained from a 4 cm section of the SF6 PCF pumped by the Cr^{4+}:YAG oscillator generating 60–70 fs pulses at 100 MHz repetition rate with the average output power of up to 170 mW [33]. The typical observed infrared and TH spectra are shown in Figs. 3,4. Fig. 4 demonstrates the TH spectrum together with its decomposition according to the multimode phase matching scheme presented in Fig. 2. The TH spectrum can be interpreted as a multimode composite, excited by the FWM process, which is phase-matched with the infrared SC generated within the lowest modes.

Since the multimode phase matching mechanism provides a good description of the TH spectral structure, one can suppose that the intra-fiber power is not too high or/and that the TH radiation losses are sufficiently strong in order to suppress the contribution of the cross-phase modulation to the mode matching. In the general case, such a conclusion would not be valid [27] and one can see the effect of the cross-phase modulation on the TH spectrum in the numerical simulation below.

Intensities of the TH spikes are defined by several factors including the SC dynamics at the fundamental wavelength as discussed in the next section. Another important contribution comes from the mode spatial structure, because various modes will have different overlapping with the pump mode (affects FWM efficiency) and different waveguide radiation losses (propagation attenuation). Both overlapping factor and radiation losses were found numerically on the basis of the generalized eigenvalue method [33]. The overlapping factors of the most intense modes m_{74} (Fig. 1) and m_{75} are 12% and 14%, and the radiation losses are 9 and 20 dB/m, respectively. As another example, the radiation loss for the weaker mode m_{71} with comparable overlapping factor is ≈2000 dB/m (leaking mode). Another leaking mode m_{73} contributes in the right maximum spike together with m_{74}. One can conclude that the TH spectrum shape depends on both overlapping factor and radiation losses for the excited modes.

PCF with 2.5 μm core provides a higher effective nonlinearity due to its small effective mode area (A_{eff}=3.7 μm^2 for the lowest-order mode). As a result, the FWM efficiency is higher than in

#83343 - $15.00 USD Received 24 May 2007; revised 19 Jul 2007; accepted 15 Aug 2007; published 22 Aug 2007

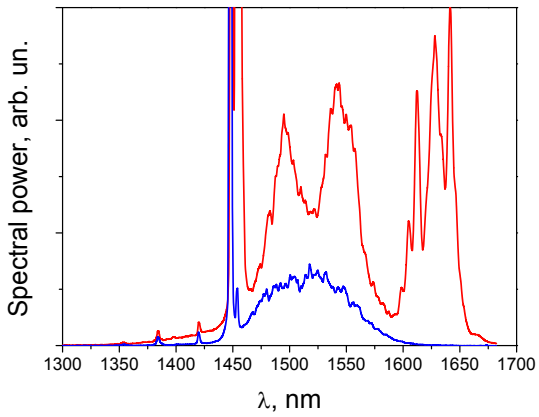

Fig. 3. Experimental SC spectrum (red) from the SF6 PCF with a 2.5 μm core. Blue curve shows the spectrum of the input pulse. The spectrometer resolution was 1.4 nm.

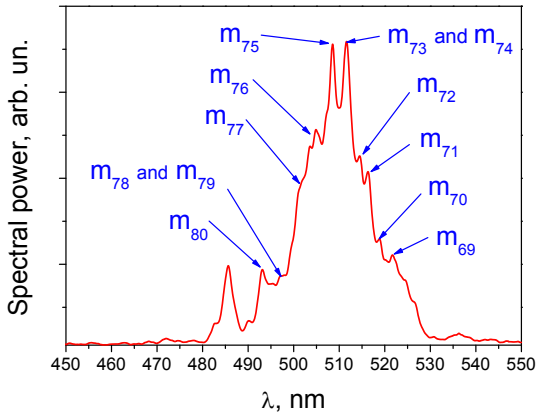

Fig. 4. Experimental TH spectrum from the SF6 PCF with a 2.5 μm core and its mode decomposition according to from Fig. 2. The spectrometer resolution was 0.5 nm

the case of the larger core sizes (e.g. A_{eff}=9.4 μm^2 for the lowest-order mode of a PCF with 4.5 μm core). This fact is easily observable in the experiment. However, since the zero-dispersion wavelength is $\lambda \approx$1.2 μm for the small core PCF, the SC spectrum is smooth and comparatively narrow [33]. The 4.5 μm core PCF produces TH with lower intensity, but i) its density of high-order modes is higher around $\lambda_0/3$ (Fig. 5) and ii) its SC is wider and more modulated due to the proximity of the zero-dispersion wavelength to λ_0. The latter is most interesting for an analysis because it affects the TH temporal structure and dynamics.

3. Spatial, spectral and temporal structures of TH

For the 4.5 μm core PCF the zero-dispersion wavelength is close to $\lambda_0 \approx$ 1.5 μm. This provides a comparatively wide SC shown in Fig. 6. Its spectral structure can be interpreted as consisting of i) the soliton spike centered at 1.6 μm, ii) the auto-modulated remainder of the pump pulse at 1.5 μm (narrow line is the cw component from the oscillator), iii) the dispersion wave at $\approx$1.26 μm, and iv) the TH spikes in the vicinity of 505 and 540 nm.

Since the TH signal is generated by the broadband SC pump pulse, many modes are generated simultaneously. This results in a broad almost featureless spectrum (Fig.6), as well as

#83343 - $15.00 USD Received 24 May 2007; revised 19 Jul 2007; accepted 15 Aug 2007; published 22 Aug 2007

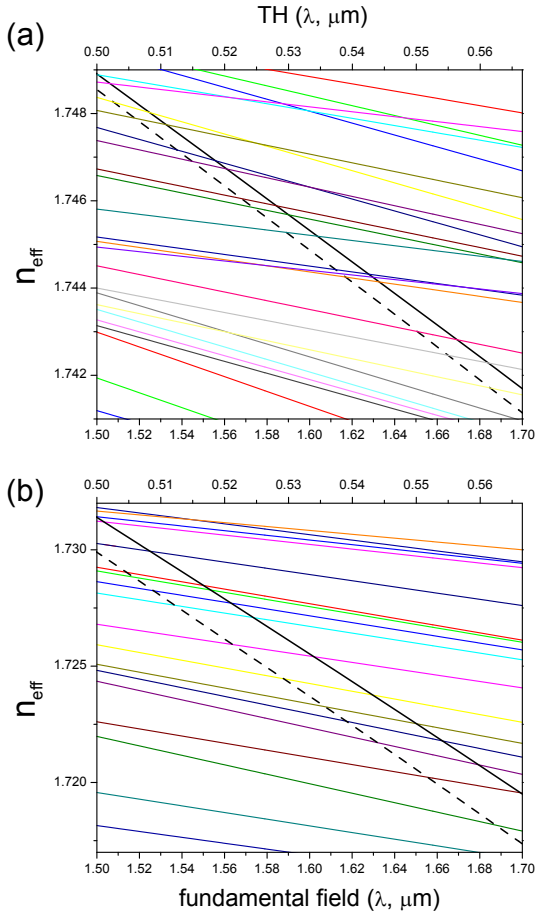

Fig. 5. Effective index of refraction $n_{\mathrm{eff,M}}$ for modes at fundamental wavelength: (a) M=1 (solid black), M=2 (dashed black); (b) M=3 (solid black), M=4 (dashed black). Colored lines show the effective indices of refraction for the third harmonic modes ($\approx \lambda_0/3$, modes are not enumerated). SF6 PCF with 4.5 μm core.

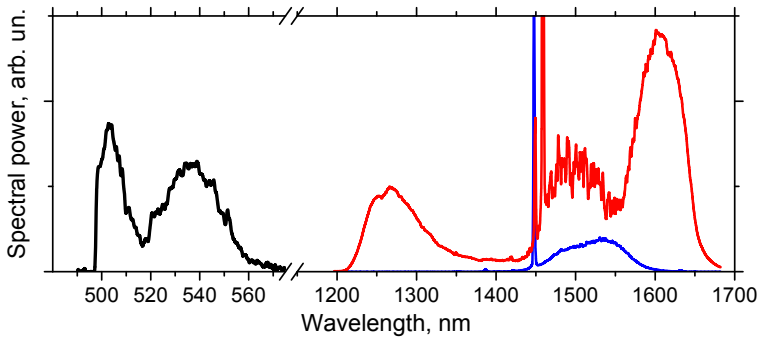

Fig. 6. Experimental spectra of the SC (red) and TH (black) from SF6 PCF with 4.5 μm core. Blue curve shows the input pulse spectrum. All three spectra are normalized separately for better visibility.

#83343 - $15.00 USD Received 24 May 2007; revised 19 Jul 2007; accepted 15 Aug 2007; published 22 Aug 2007

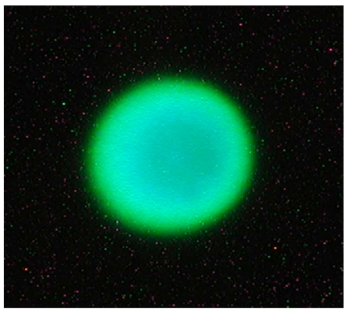

Fig. 7. Intensity profile of the TH radiation from the 4.5 μm core of SF6 PCF, taken at approximately 3 cm free propagation distance after the fiber end. The individual mode patterns can not be resolved.

smooth structureless mode pattern at the output (Fig.7), which is an overlap of many mode patterns (Fig. 1) with close wavelengths. Such an overlap develops already at the initial propagation stage and the individual modes cannot be resolved. In similar experiments with fused silica-based PCFs and tunable narrowband pump pulses one can observe and resolve the individual phase-matched high-order modes [17], which are also conveniently separated from each other due to the lower mode density in the 2.5 μm-core fused silica as opposed to the 4.5 μm-core SF6.

To analyze the SC dynamics numerically, we reduce the full 3+1 dimensionality to 1+1-dimensional problem for each pair of modes (one lowest-order pump mode and one high-order mode at $\lambda_0/3$). We also approximate the slightly birefringent PCF core by a core with cylindrical symmetry and 5.2 μm diameter, providing the same zero-dispersion wavelength at ≈ 1.5 μm. Spatial profiles of the three high-order modes providing the phase-matching with the infrared SC are shown in Fig. 8. The mode structure of the cylindrical core differs from that of the experimental PCF. Therefore, the TH spectral structure can be reproduced only approximately. In particular, the birefringence effects disappear and there are 4 times less phase-matching points (only three in the wavelength interval 450–600 nm). In the rest of the paper we concentrate on the TH dynamics and its co-evolution with the supercontinuum.

The model which describes an interaction between the fundamental (SC, a_F) and third harmonic (a_{TH}) fields is based on the slowly varying amplitude approximation, which is valid for our pulse width (the case of the extremely short pulses is considered in [31, 32]). The equations consider the fields separately but with the coupling through FWM [8, 21, 22, 20, 35]:

$$\frac{\partial a_F}{\partial z} = -\frac{i}{2}\beta_2(\omega-\omega_F)\frac{\partial^2 a_F}{\partial t^2} + i\gamma_F\left(1+\frac{i}{\omega_F}\right)\left\{\left[|a_F|^2+2\xi|a_{TH}|^2\right]a_F + \xi a_F^{*2}a_{TH}\exp(iz\Delta k)\right\},$$
$$\frac{\partial a_{TH}}{\partial z} = -\frac{i}{2}\beta_2(\omega-\omega_{TH})\frac{\partial^2 a_{TH}}{\partial t^2} - \delta\frac{\partial a_{TH}}{\partial t} + i\gamma_{TH}\left(1+\frac{i}{\omega_{TH}}\right)\times \quad (1)$$
$$\left\{\left[|a_{TH}|^2+2\xi|a_F|^2\right]a_{TH} + \xi a_F^3\exp(-iz\Delta k)\right\}.$$

Here z is the propagation distance, t is the local time (frame of reference is co-moving with the group velocity v_F of the fundamental field at $\omega_F = 2\pi c/\lambda_0$), $\omega_{TH} = 3\omega_F$, $\Delta k = (\omega_{TH}-\omega_F)/c$, $\gamma_F = n_2\omega_F/cA_{\text{eff}}^F$, $\gamma_{TH} = n_2\omega_{TH}/cA_{\text{eff}}^{TH}$, $\delta = v_F - v_{TH}/v_F v_{TH}$, n_2 is the nonlinear refractive index, c is the velocity of light. A_{eff}^F and A_{eff}^{TH} are the effective mode areas at ω_F and ω_{TH}, respectively. Parameter β_2 describes the frequency-dependent GDD in the vicinity of ω_F (first equation) or ω_{TH} (second equation). Parameters v_F and v_{TH} are the group velocities at ω_F and

#83343 - $15.00 USD Received 24 May 2007; revised 19 Jul 2007; accepted 15 Aug 2007; published 22 Aug 2007

ω_{TH}, respectively. The overlapping of modes [36] at ω_F and ω_{TH} defines the parameter ξ. TH initial filed is assumed null $a_{TH}(z=0)=0$.

The spectral profile of $\beta_2(\omega)$ reproduces the fiber dispersion and includes the contribution of high-order dispersions up to the 12^{th} order. Taking into account of the higher-order dispersions is necessary to describe the SC structure and its dynamics, which affects the TH.

Numerical simulations were performed pairwise between the fundamental and each higher-order modes. Such an approach is valid in our case because the energy conversion into TH is small (Fig. 11).

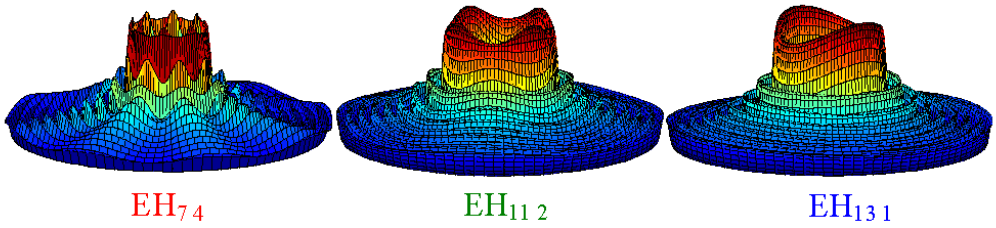

Fig. 8. Spatial profiles of the three TH modes in the cylindrical 5.2 μm core of the SF6 PCF.

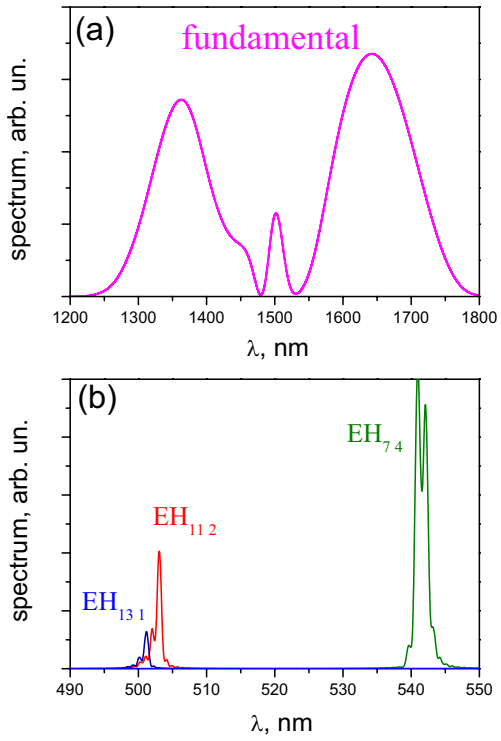

Fig. 9. Calculated: the SC (a) and the TH (b) spectra for the modes of Fig. 8.

The simulations confirm that the signal in the higher-order modes appears in the vicinity of the tripled pump wavelength at $\lambda \approx \lambda_0/3$ and $\Delta k \approx 0$ [11]. As new wavelengthes are being generated in the infrared SC along the propagation coordinate (within both solitonic and

#83343 - $15.00 USD Received 24 May 2007; revised 19 Jul 2007; accepted 15 Aug 2007; published 22 Aug 2007

dispersion-wave parts of SC), the phase-matched TH higher-order modes grow in the form of isolated spectral spikes [18]. Fig. 9 shows three modes with the highest simulated intensity. They correspond to initial Δk close to 0. The spikes have widths of the order of few nanometers. There is a spectral overlap between some TH modes. The spectra have a fine structure and asymmetry [27, 28], resulting from the cross-phase modulation with the fundamental wave. The cross-phase modulation is hardly visible in the experiment because of the radiation losses. In the numerical simulation, where we neglect the radiation losses, the cross-phase modulation effect is stronger.

Fig. 10 shows the instantaneous snapshot of the co-propagating signals at a fiber length of 4 cm. Because of the large group velocity difference, the TH wave is constantly retarded from the SC pulse. In the calculation, the local time frame is moving with a constant velocity, which is equal to the group velocity of the input pulse at 1.5 μm, and is close to the group velocity of the SC signal. Plotting the temporal intensity profile of the TH signal in the local time frame thus shows a generation history of the TH signal during the propagation.

It is interesting to note, that at the beginning of the TH generation there are ripples with a period of the order of ~ 100 fs (Fig. 10b). The reason for this can be understood, if we take into account, that at the initial stage, the frequency of the TH signal is exactly $\omega_{TH} = 3\omega_F$. For most of the high-order modes, this is not the phase-matched frequency, and the signal shows typical oscillations of the non-phase-matched harmonic generation with $\Delta k \neq 0$. Later on, in the first few millimeters of propagation [34], the spectrum expansion takes place, and the TH generation frequency shifts to the perfect phase-matching $\Delta k = 0$.

The long-term modulation of the TH temporal profile (≈ 10 ps, Fig. 8a) results from the variation of the SC spectral power at the phase-matched wavelengths along the propagation distance z. A combination of the short-scale (due to $\Delta k \neq 0$) and long-scale (due to the SC evolution) modulations creates the unique temporal structure of the TH signal. Note that the long-scale evolution is mode-dependent (Fig. 8), because it is connected with the SC intensity evolution at the tripled wavelength of the mode-specific phase-matching point.

Finally, Fig. 11 shows the evolution of the overall energy in the TH modes as a fraction of the input pulse energy. At 4 cm propagation length, the maximum conversion efficiency is $\sim$0.8%. This value is likely the upper estimation of the conversion efficiency, because the model does not account for the radiation losses of the high-order TH modes.

4. Conclusion

Multimode phase-matched four-wave-mixing providing the third-harmonic generation in microstructured fibers has been explored numerically taking into account the propagation dynamics within the framework of slowly-varying amplitude approximation. It has been found, that the the TH signal is a superposition of spectral peaks, which are excited in the high-order spatial modes providing the phase matching with the supercontinuum in the PCF. The calculated TH peaks and SC spectra are in a good agreement with the experimental ones, which have been obtained from the SF6 glass PCF pumped by a femtosecond pulse Cr^{4+}:YAG oscillator. The structure of the experimental TH spectrum is completely described by the multimode phase-matching conditions in the actual geometry of the PCF core.

Temporal structure of the TH has been analyzed in connection with the SC dynamics. The TH appears in the vicinity of the tripled pump frequency in the form of isolated spectral lines propagating in the modes with $\Delta k \neq 0$. Imperfect phase-matching causes the TH envelope ripples with the sub-picosecond period. Such ripples decay when the SC approaches the perfect phase-matching frequency, where $\Delta k \to 0$. After that the temporal structure of TH is affected mainly by the dynamics of SC. The resulting TH signal has the form of a intensity-modulated pulse with approximately 10-ps duration, which stretches out of the SC pulse due to the differ-

#83343 - $15.00 USD Received 24 May 2007; revised 19 Jul 2007; accepted 15 Aug 2007; published 22 Aug 2007

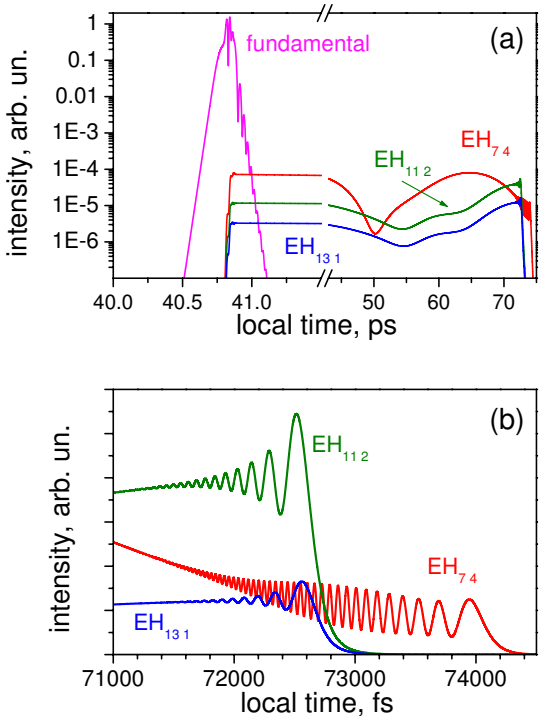

Fig. 10. Calculated: SC (fundamental) and TH temporal profiles for the modes of Fig. 6 at 4 cm propagation length. (a) Full time window of the TH signal (log scale). (b) Trailing edge of the TH pulse, corresponding to the beginning of the TH generation (linear scale).

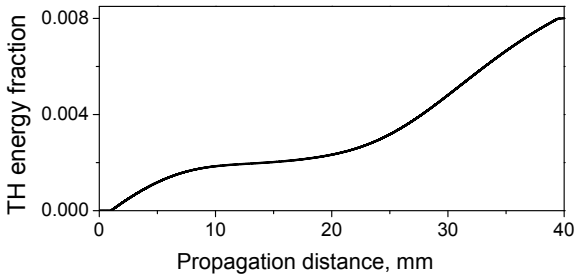

Fig. 11. Calculated evolution of the total TH energy fraction for the modes of Fig. 8.

#83343 - $15.00 USD Received 24 May 2007; revised 19 Jul 2007; accepted 15 Aug 2007; published 22 Aug 2007

ence between the SC and TH group velocities.

Acknowledgements

The supercontinuum and third-harmonic spectra have been obtained in collaboration with S. Naumov using the SF6 fibers provided by J. Knight from the University of Bath. This work was supported by the Austrian National Science Fund (FWF), project P17973-N08.

#83343 - $15.00 USD Received 24 May 2007; revised 19 Jul 2007; accepted 15 Aug 2007; published 22 Aug 2007